INSTITUTE OF PHYSICS PUBLISHING JOURNAL OF OPTICS B: QUANTUM AND SEMICLASSICAL OPTICS

J. Opt. B: Quantum Semiclass. Opt. **6** (2004) S265–S270 PII: S1464-4266(04)72656-7

Stable droplets and nucleation in asymmetric bistable nonlinear optical systems

Damià Gomila[1], Pere Colet[2], Gian-Luca Oppo[1] and Maxi San Miguel[2]

[1] Department of Physics, University of Strathclyde, 107 Rottenrow East, Glasgow G4 0NG, UK

[2] Instituto Mediterráneo de Estudios Avanzados (IMEDEA, CSIC-UIB), Campus Universitat Illes Balears, E-07122 Palma de Mallorca, Spain[3]

E-mail: damia@phys.strath.ac.uk

Received 26 November 2003, accepted for publication 23 February 2004
Published 4 May 2004
Online at stacks.iop.org/JOptB/6/S265
DOI: 10.1088/1464-4266/6/5/014

Abstract

The existence and stability properties of localized structures in nonlinear optical cavities with slightly non-equivalent homogeneous solutions and displaying a modulational instability of flat fronts are investigated. We present a new type of stable localized structures in the regime of formation of labyrinthine patterns based on the balance between the curvature and the asymmetry effects.

Keywords: nonlinear optical cavities, transverse effects, localized structures, domain walls, cavity solitons, pattern formation

(Some figures in this article are in colour only in the electronic version)

1. Introduction

The formation of localized structures in the transverse plane of nonlinear optical cavities has been studied in several systems in recent years [1]. Two kinds of cavity solitons have been extensively considered, those arising in regimes where a spatially modulated solution coexist with an homogeneous one [2] and those associated with the existence of two equivalent stable homogeneous solutions (also referred to as phases). Analogously, in systems with a quadratic nonlinearity, two homogeneous solutions may differ from each other by a π phase shift in the slowly varying amplitude of the electric field and still be completely equivalent from the dynamical point of view. In systems with polarization symmetry two homogeneous solutions with different polarization states are dynamically equivalent. Cavity solitons in these systems in two transverse dimensions are often formed by shrinking domains of one phase surrounded by the other. The domain walls separating the two equivalent phases are narrow spatial features [3] and present damped oscillations in their tails due to diffraction. When a domain of one phase or polarization embedded in the other shrinks, these oscillatory tails interact and may form stable localized states. The intensity profile of these cavity solitons is characterized by a peak surrounded by a dark ring and then by a homogeneous phase. Dark ring cavity solitons (DRCSs) have been described first in the mathematical context of the Swift–Hohenberg equation [4] and later in the degenerate optical parametric oscillator (DOPO) both off [5] and at resonance [6, 7], in non-mean field models [8] and in the vectorial Kerr resonator [9].

More recently, we have described a different kind of stable localized structures with wide relevance in nonlinear optics: the stable droplet (SD) [10, 11]. In contrast with DRCSs, whose size is typically of the order of a domain wall width and with central peak intensity larger than the corresponding homogeneous solution, SDs are large stable circular domain walls separating the two homogeneous solutions. SDs in symmetric bistable systems appear close to the modulational instability of a flat domain wall and balance the curvature-driven shrinking of a domain with the growth due to the instability of tightly curved fronts [10]. There is a fundamental

[3] http://www.imedea.uib.es/physdept

difference between the mechanism that allows for the existence of previously reported localized structures, namely cavity solitons in regimes where a homogeneous and a spatially modulated solution coexist and cavity solitons are stabilized by oscillatory tail interaction (DRCS), and the SD. While the first two types of cavity solitons exist both in one and two dimensional systems, SDs have no counterpart in 1D since their stability is due to curvature effects. Therefore they only exist in systems whose dimensionality is at least two. The SD has been described both in a generic prototype equation, the parametrically driven complex Ginzburg–Landau equation (PCGLE) [10], as well as in specific models of nonlinear optics devices such as the DOPO and vectorial Kerr resonators with linearly polarized pump [11].

In real photonic systems the assumption of two exactly identical phases can be considered as an idealization. A small symmetry breaking in the field phases can appear due to small higher order nonlinear terms or be induced by a small external seeding. Similarly a residual birefringence or a pump with a slight elliptical polarization can break the polarization symmetry. As soon as the symmetry is broken the homogeneous solutions become dynamically non-equivalent. In one dimensional systems a front connecting these two solutions will move in a given direction. The direction of the motion provides an indication of which is the most stable solution after the breaking of the symmetry. In two dimensional systems curvature comes into play and therefore a competition between curvature and drift may arise. In systems approaching thermodynamical equilibrium this scenario has been studied within the so-called nucleation theory [12]. It is well known that an equilibrium radius at which curvature effects and drift counterbalance each other exists. However, this localized structure (labelled as 'nucleus' in the following) is typically unstable and either grows to infinite size or shrinks until it disappears. In this paper we analyse the effects of a small symmetry breaking on the existence of localized structures in a general class of two dimensional nonlinear systems. We show for example that in regimes of labyrinthine pattern formation, an equilibrium between the drift due to the asymmetry and local curvature leads to the formation of a new kind of SD. Labyrinthine patterns have been observed for instance in nonlinear chemical reactions [13], and they are commonplace in nonlinear optics [9, 14, 15]. Our results follow from an extension of the analysis given in [10]. For this reason, we review the general results for SDs in symmetric bistable systems in section 2, with particular emphasis on their relevance in nonlinear optics. Section 3 is devoted to the general theory of SDs in two dimensional asymmetric bistable systems displaying a modulational instability of stable fronts. The application of the general theory to the cases of the solution inside the circular domain being favoured or disfavoured by the asymmetry are presented in sections 4 and 5. In the first case, before the modulational instability of the front the nucleus merges directly from an SD or a DRCS, while in the second case curvature and front motion balance to originate an SD after the instability. For convenience and generality we apply the theory to the PCGLE equation with diffusion and diffraction. Our results, however, are universal in nonlinear optics and we present evidence of SDs in the labyrinthine regime in an asymmetric singly resonant DOPO in section 5. Conclusions are presented in section 6.

2. Stable droplets in nonlinear optical systems with phase or polarization symmetry

In this section we briefly review the origin and properties of SDs in symmetric bistable systems with emphasis on their relevance in nonlinear optics. SDs exist close to modulational instabilities of a stable front separating two stable homogeneous phases or polarization domains[4]. Before and away from the front instability, circular domains of one phase (polarization) surrounded by the other shrink to zero radius due to local curvature effects. Such shrinking may be stopped by DRCSs because of the interaction of the tails of the curved fronts [10, 11] or by the presence of other localized states [16]. Beyond the modulational instability of the front, however, circular domains grow to infinite size. For intermediate values of the control parameter, an equilibrium between the large radius shrinking droplets where curvature effects dominate and small radius expanding droplets where the tight front instability prevails is found. SDs are then formed which correspond to stable circular domains [10, 11]. In particular we showed that SDs exist for spatially extended dynamical systems in two dimensions and of the form

$$\partial_t \vec{\Psi} = D\nabla^2 \vec{\Psi} + \vec{W}(\vec{\Psi}, p), \tag{1}$$

where $\vec{\Psi}(\vec{x})$ is a real N component vector field, the matrix D describes the spatial coupling, $\vec{W}$ is a local nonlinear function of the fields and p a control parameter. Equation (1) is invariant under translations and under the change $\vec{x} \to -\vec{x}$. In addition we assume that it has a discrete symmetry $\mathcal{Z}$ that allows for the existence of two, and only two, equivalent stable homogeneous solutions, and that, in a 1D system, they are connected by a stable Ising front $\vec{\Psi}_0(x, p)$ (see footnote 4). An Ising front satisfies

$$\vec{\Psi}_0(x_0 - x) = \mathcal{Z}\vec{\Psi}_0(x - x_0), \tag{2}$$

where x_0 is the front location [17] so that the 1D front (and equivalently a flat front in 2D) is stationary, $D\nabla^2\vec{\Psi}_0 + \vec{W}(\vec{\Psi}_0, p) = 0$. The modulational instability of the front is identified by the change of sign of the quantity

$$\gamma(p) \equiv \frac{1}{\Gamma}\int_{-\infty}^{\infty} \vec{a}_0 \cdot D\vec{e}_0 \, \mathrm{d}r, \tag{3}$$

where $\vec{e}_0 \equiv \partial_r \vec{\Psi}_0$ is the Goldstone mode of the front and $\Gamma \equiv \int_{-\infty}^{\infty} \vec{a}_0 \cdot \vec{e}_0 \, \mathrm{d}r$[Note 5], and $\vec{a}_0$ is the null mode of $M^\dagger$ with $M^i_j = D^i_j \partial_r^2 + \delta_{\Psi^j} W^i|_{\vec{\Psi}_0, p}$ being the operator of the linearization around the flat front. For a circular domain of radius R the curvature is equal to $1/R$, while the (normal) front velocity v is

$$v = \partial_t R = -\gamma(p)/R. \tag{4}$$

Marking with p_c the value of the control parameter at the front instability, one clearly sees from (4) that before the instability ($\gamma > 0$ for $p > p_c$) large domains shrink, while

[4] This work and that presented in [10, 11] is concerned specifically with Ising walls and avoids parameter regions where Ising–Bloch transitions and Bloch walls exist.

[5] Γ vanishes at an Ising–Bloch transition [17]. Here we only consider parameter regions far away from any Ising–Bloch transition for which Γ is never zero.

after the instability ($\gamma < 0$ for $p < p_c$) circular domains diverge to infinity. A multiple scale analysis of circular domains, however, reveals that for $\gamma > 0$ (i.e. $p > p_c$), the initial shrinking of large domains can be counterbalanced by a growth of small radius domains due to the incoming front instability. In particular the radius of the circular domain obeys the equation

$$\partial_t R = -c_1(p - p_c)\frac{1}{R} - c_3\frac{1}{R^3}, \tag{5}$$

where the coefficients $c_1 = \gamma/(p - p_c)$ and c_3 are model dependent and can be evaluated exactly once the form of the equation (1) is given [10]. Since $c_1 > 0$, SDs of radius

$$R_0 = \frac{1}{\sqrt{p - p_c}}\sqrt{\frac{-c_3}{c_1}}. \tag{6}$$

form when c_3 is negative. Equation (5) clearly shows that SDs in symmetric bistable systems are due to the balance of the curvature (the c_1 term) and the instability of tightly curved fronts (the c_3 term) which dominated the dynamics at the front instability ($\gamma = 0$ and $p = p_c$).

We verified the validity of this general theory in three different models. First, in the PCGLE in the presence of both diffusion and diffraction [10]

$$\partial_t A = (1 + \mathrm{i}\alpha)\nabla^2 A + (\mu + \mathrm{i}\nu)A - (1 + \mathrm{i}\beta)|A|^2 A + pA^*, \tag{7}$$

where α is the ratio between diffraction and diffusion, μ measures the distance from the oscillatory instability threshold, ν is the detuning and $p > 0$ is the forcing amplitude. In [10] we used the PCGLE as a generic model displaying both labyrinths and SDs. We note, however, that specific limits of this equation have found direct application in modelling optical devices. For example, the PCGLE with zero diffusion, $\mu = -1$ and $\beta = 0$ describes a singly resonant DOPO where the pump field is not resonated [7, 18, 19]. The PCGLE with zero diffusion, $\mu = -1$ and purely imaginary nonlinear coefficient (more correctly referred to as the parametrically driven nonlinear Schrödinger equation; see [16] for general results) describes DOPO with large pump detuning [3, 20] and vectorial Kerr resonators with large cavity anisotropy [21]. In [10] we located an entire branch of SD solutions for $p > p_c = 2.566\,29$ for $\alpha = 2$, $\beta = 0$, $\nu = 2$ and $\mu = 0$. It is important to note that SDs are generic to parameter changes provided that a modulational instability of the front is detected.

In [11] we verified the existence of SDs in a model for a vectorial Kerr resonator [22]:

$$\begin{aligned}\partial_t E_\pm = &-(1 - \mathrm{i}\theta)E_\pm + \mathrm{i}\nabla^2 E_\pm + E_0 \\ &- \tfrac{1}{4}\mathrm{i}[|E_\pm|^2 + \beta|E_\mp|^2]E_\pm,\end{aligned} \tag{8}$$

where $E_\pm$ are the circularly polarized field components, E_0 is the pump (x-polarized), θ is the cavity detuning, ∇^2 is the transverse Laplacian, and β is related to the susceptibility tensor. We found SDs for $E_0 > E_c = 1.550$, $\theta = 1$, and $\beta = 7$. Finally, SDs were described in the DOPO model

$$\begin{aligned}\partial_t A_0 &= \Gamma[-A_0 + E_0 - A_1^2] + \frac{\mathrm{i}a}{2}\nabla^2 A_0 \\ \partial_t A_1 &= -A_1 - \mathrm{i}\Delta_1 A_1 + A_0 A_1^* + \mathrm{i}a\nabla^2 A_1,\end{aligned} \tag{9}$$

where A_0 and A_1 are the pump and signal field, Γ is the ratio between the pump and signal cavity decay rates, E_0 is the amplitude of the external pump field (our control parameter), Δ_1 is the signal detuning, and a is the diffraction parameter. Again, SDs were found for $E_0 > E_c = 2.189$, $\Gamma = 6$, $a = 0.5$, and $\Delta_1 = -1$ [11]. An intriguing bistability between an SD and a DRCS was also described.

3. General theory of stable nucleation droplets in systems with asymmetry

As stated in the introduction, our theoretical work is presented in the general framework developed in [10]. Therefore, we consider a generalization of (1) to systems with asymmetry

$$\partial_t \vec{\Psi} = D\nabla^2\vec{\Psi} + \vec{W}(\vec{\Psi}, p) + \epsilon\vec{S}, \tag{10}$$

where $\epsilon\vec{S}$ is a symmetry breaking term. For $\epsilon \neq 0$ the two homogeneous solutions are no longer equivalent; the 1D Ising front does not satisfy the symmetry condition (2) and therefore it moves.

Assuming that the asymmetry is small ($\epsilon \ll 1$) and proceeding as in [10], we derive an equation for the evolution of a circular domain of one phase surrounded by the other. In cylindrical coordinates (r, θ) and in the reference frame moving with the front, equation (10) becomes

$$D\partial_r^2\vec{\Psi} + \left(\dot{R}I + \frac{1}{R}D\right)\partial_r\vec{\Psi} + \frac{1}{R^2}D\partial_\theta^2\vec{\Psi} + \vec{W}(\vec{\Psi}, p) + \epsilon\vec{S} = \partial_t\vec{\Psi}, \tag{11}$$

where R is the radius of the circular domain and $\dot{R}$ its radial velocity. We analyse the dynamics of radially symmetric fronts ($\partial_\theta\vec{\Psi} = 0$) with a large radius ($R \gg 1$). We also assume that in the moving reference frame the front profile is stationary ($\partial_t\vec{\Psi} = 0$). Linearizing around the stationary profile $\vec{\Psi}_0$ of the symmetric ($\epsilon = 0$) 1D front we obtain the following equation for the perturbation $\vec{\Psi}_1 = \vec{\Psi} - \vec{\Psi}_0$:

$$M\vec{\Psi}_1 = -\epsilon\vec{S} - \left(\dot{R}I + \frac{1}{R}D\right)\partial_r\vec{\Psi}_0, \tag{12}$$

where $M^i_j = D^i_j\partial_r^2 + \delta_{\Psi^j}W^i|_{\vec{\Psi}_0, p}$ is the Jacobian of equation (10). Due to the translational invariance of (10), now broken by the presence of the front, each front has a neutrally stable mode $\vec{e}_0$, namely $M\vec{e}_0 = \vec{0}$. This mode is known as the Goldstone mode, and it has the form of the gradient of the front $\vec{e}_0 \equiv \partial_x\vec{\Psi}_0$. M is therefore a singular matrix, so there exists a solvability condition for equation (12) which is obtained by multiplying on the left both sides of (12) by the null vector of $M^\dagger$, $\vec{a}_0$. We obtain

$$\dot{R} = v_0(p) - \gamma(p)\frac{1}{R}, \tag{13}$$

where

$$v_0(p) = -\epsilon\frac{1}{\Gamma}\int_{-\infty}^{\infty}\vec{a}_0 \cdot \vec{S}\,\mathrm{d}r, \tag{14}$$

and $\gamma(p)$ is given by (3). $v_0(p)$ corresponds to the velocity of the 1D front connecting the two homogeneous solutions and vanishes for $\epsilon = 0$. $v_0(p)$ is positive if the inner solution is more 'stable' and negative otherwise. $\gamma(p)$ is the coefficient of the curvature driven term and is independent of the symmetry

breaking term ϵ. We remark here that the expression $\gamma(p)$ is the same as for the systems with phase and polarization symmetry discussed in section 2. Both $v_0(p)$ and $\gamma(p)$ depend on the control parameter p through the shape of the symmetric 1D front $\vec{\Psi}_0$. Typically, the dependence of v_0 on the system parameters is quite weak, while off-diagonal terms in D may induce a quite strong dependence on the parameters in γ. This is of particular relevance in nonlinear optical systems where the spatial coupling is diffractive and therefore D only contains off-axis elements. We have already seen in section 2 that γ can easily change its sign at $p = p_c$ for several models in nonlinear optics. This means that for $\gamma > 0$ ($\gamma < 0$) the curvature effect tends to shrink (grow) circular domains and a flat front is stable (unstable). If v_0 and γ have the same sign, equation (13) predicts an equilibrium radius R_0 for which the curvature effect is exactly compensated by the radial motion of the front due to the asymmetry of the homogeneous solution

$$R_0 = \frac{\gamma}{v_0} = -\frac{1}{\epsilon}\frac{\int_{-\infty}^{\infty} \vec{a}_0 \cdot D\vec{e}_0 \, \mathrm{d}r}{\int_{-\infty}^{\infty} \vec{a}_0 \cdot \vec{S} \, \mathrm{d}r}. \qquad (15)$$

It is important to stress that the circular localized structures corresponding to (15) are closely related to the SDs presented in section 2 but are stabilised by a different mechanisms where the role of the asymmetry ϵ is essential. In the following two sections we discuss the cases of $v_0 > 0$ and $v_0 < 0$ separately.

4. Nucleation for $v_0 > 0$

This case corresponds to the situation in which the inner solution of the circular domain is favoured by the asymmetry. For $p > p_c$ ($\gamma > 0$) the domain wall dynamics is qualitatively described by the so-called nucleation theory of fronts in potential systems with two stable phases with different stability [12]. It is well known that in 1D the fronts move with a velocity proportional to the potential difference between the two solutions, and that in 2D the surface tension may counterbalance the potential difference leading to a stationary circular domain (nucleus). It is also well known that this nucleation radius is always unstable, and a circular domain with a larger radius grows until infinity and a domain with a smaller radius shrinks until it disappears. For the systems that we are considering here, there is no known potential. We can, however, consider γ as an effective 'surface tension' and describe the dynamics as in nucleation theory. When γ is positive and large the equilibrium radius (15) is very large.

We have studied the nucleation regime for $v_0 > 0$ in the asymmetric PCGLE [23]

$$\partial_t A = (1+\mathrm{i}\alpha)\nabla^2 A + (\mu+\mathrm{i}\nu)A - (1+\mathrm{i}\beta)|A|^2 A + pA^* + \epsilon. \quad (16)$$

The dashed line in figure 1 is the radius of the nucleation droplet for the asymmetric PCGLE (16) obtained numerically by solving the stationary radial equation

$$(1+\mathrm{i}\alpha)\left(\partial_r^2 + \frac{1}{r}\partial_r\right)A + (\mu+\mathrm{i}\nu)A - (1+\mathrm{i}\beta)|A|^2 A + pA^* + \epsilon = 0. \qquad (17)$$

The dotted line in figure 1 shows the radius of the nucleation droplet from the theoretical prediction (15). The 1D front profile $\vec{\Psi}_0$ is obtained by solving the 1D stationary equation

$$(1+\mathrm{i}\alpha)\partial_r^2 A + (\mu+\mathrm{i}\nu)A - (1+\mathrm{i}\beta)|A|^2 A + pA^* = 0. \quad (18)$$

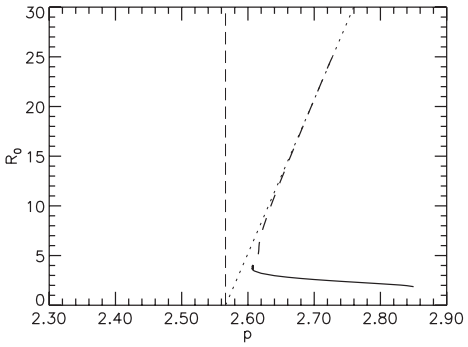

Figure 1. Radius of the nucleation droplet (dashed line) and DRCS (solid line) as a function of p. The dotted line corresponds to the theoretical prediction (15) while the solid (dashed) line has been obtained by numerically solving the stationary radial equation (17). The DRCS is stable, while the nucleation droplet is always radially unstable. Here we have taken $\alpha = 2$, $\beta = 0$, $\nu = 2$, $\mu = 0$ and $\epsilon = 5 \times 10^{-2}$. The vertical dot–dashed line indicates the modulational instability point $p_c = 2.566$ of a flat wall in 2D.

Both equations (17) and (18) have been solved by means of a Newton method in which the space has been discretized and the transverse derivatives computed in Fourier space [7, 24]. To compute (15) we also evaluate the operator M, which now takes the form of an $N \times N$ matrix where N is the number of grid points, from the discretized profile $\vec{\Psi}_0$. The null mode of $M^\dagger$ is easily obtained by finding the eigenvalues and eigenmodes of the transposed of the matrix M.

When p decreases, γ also decreases, making R_0 smaller. The agreement between the theoretical prediction (15) and the numerically evaluated radius for the nucleation droplets is excellent until R_0 becomes too small and the approximations used to obtain (12) are no longer valid. This happens when R_0 becomes of the order of the front width. In fact, this distance is also the range of the oscillatory tail interactions which may stop the shrinking due to the curvature leading to the formation of DRCSs. The radius of the DRCS obtained by solving numerically the radial equation (17) is also shown in figure 1 with a solid line. The branch of nucleation droplets connects, close to p_c, with the branch of the DRCS which extends back until $p = 2.85$, where γ becomes too large and the oscillatory tail interaction can no longer stop the collapse.

For $p < p_c$ ($\gamma < 0$) both the asymmetry and curvature effect make the circular domains grow. We have found that in the range of parameters explored for the PCGLE, the tail interaction is not able to prevent the growth of the circular domains. Therefore a circular domain keeps growing until the boundary breaks up due to the modulational instability of the circular wall. This scenario leads finally to the formation of a labyrinthine pattern.

5. Stable droplets in labyrinthine patterns for $v_0 < 0$

This case corresponds to the situation in which the outer solution is favoured by the asymmetry. For $p > p_c$ ($\gamma > 0$) both the asymmetry and the curvature effect tend to shrink the circular domains. The interaction of the tails can however stop the collapse, leading to the creation of localized structures. However, as now the tail interaction has to compensate for the combined shrinking effect of both asymmetry and curvature,

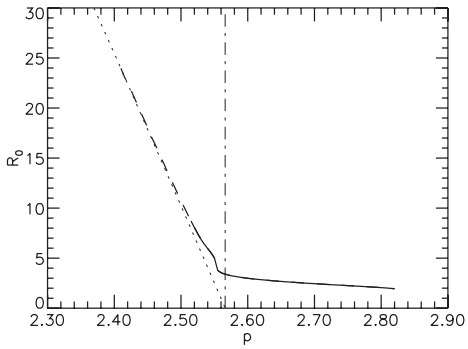

Figure 2. The radius of the stable droplet and localized structure as a function of p. The dotted line corresponds to the theoretical prediction (15) while the solid (dashed) line has been obtained by numerically solving the stationary radial equation (17). Here the solid (dashed) line refers to stable (azimuthally unstable) structures. The vertical dot–dashed line indicates the modulational instability point p_c of flat fronts.

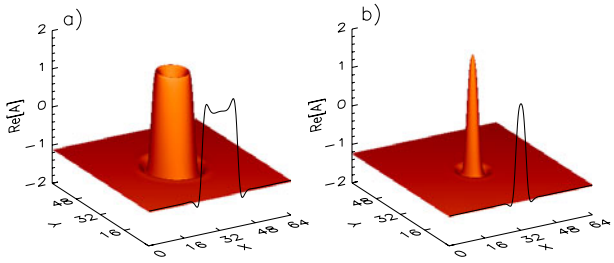

Figure 3. The real part of a stable droplet (a) and dark ring cavity soliton (b) for the PCGLE at $p = 2.52$ and 2.7. The solid curves are the central sections of the 3D plots.

the upper limit for the existence of DRCSs is shifted to $p = 2.82$, a value smaller than that shown in figure 2 in the previous section. Figure 3(b) shows the shape of a typical DRCS.

For $p < p_c$ there are now stable DRCSs, as shown in figure 2. Furthermore, there is an equilibrium radius given by (15) for which the curvature counterbalances the velocity term due to the asymmetry. In contrast to the previous case and nucleation theory, the roles of the curvature and asymmetry have been exchanged, and the equilibrium radius is stable. This leads to the existence of radially stable droplets (SDs) with a large radius beyond p_c, the threshold for the modulational instability of a flat wall in 2D, as shown in figures 2 and 3(a). While SDs are stable to radial perturbations, modulation instabilities of their circular wall in the azimuthal direction can occur. We have numerically performed a stability analysis of SDs against azimuthal perturbations of the form $\delta A = f(r)e^{im\theta}$. We find that SDs are fully stable for $p > 2.515$, as shown in figure 2. At $p = p_{m=2} = 2.515$, SDs become unstable under perturbations with azimuthal index 2 leading to the elongation of the droplet until finally a labyrinthine pattern is formed (figure 4). For lower values of the control parameter p, instabilities of larger azimuthal index dominate, as shown in figure 5 for $p = 2.46$ where an $m = 4$ instability takes place. The circular droplet evolves first towards a square shape and later to a cross whose arms keep growing until finally a labyrinthine pattern is formed.

We should emphasize, however, that in the region $p_{m=2} < p < p_c$ the SDs are fully stable. Labyrinthine patterns also

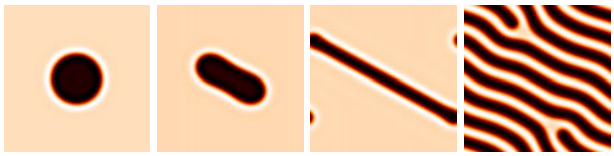

Figure 4. The $m = 2$ azimuthal instability of a droplet for $p = 2.5$. Simulations have been performed onto a 256×256 grid with $\Delta x = 0.25$. The time increases from left to right.

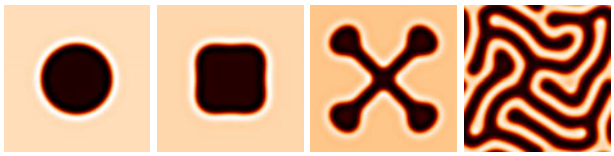

Figure 5. The $m = 4$ azimuthal instability of a droplet for $p = 2.46$.

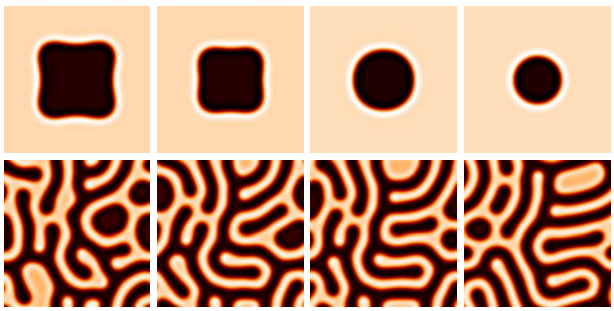

Figure 6. Evolution starting from two different initial conditions, namely a square domain (top) and random (bottom), at $p = 2.52$. Time increases from left to right. Note the formation of large elliptical-like homogeneous domains (see for instance the top right-hand corner in the formation of the labyrinthine pattern). These big bubbles are reminiscent of the existence of stable droplets, but they are deformed by the interaction with the labyrinthine pattern. The final state is frozen.

exist in the same parameter region. The evolution towards one or the other solution will depend on the initial conditions (see figure 6), and coexistence can take place.

We have also verified that these results are robust and they are present for values of the parameters more usual to systems in nonlinear optics. In particular we have verified the existence of SDs in labyrinthine patterns for the singly resonant DOPO with small injected signal (figure 7). This system is described by equations (9) in the limit of large Γ, i.e. by the PCGLE with zero diffusion, $\mu = -1$ and $\beta = 0$ [7, 18, 19].

6. Conclusions

We have studied the effect of a small symmetry breaking on the existence and stability properties of droplet-like structures due to the presence of two equivalent homogeneous states for the symmetric system. We have shown that localized structures in 2D are robust to small symmetry breakings, although their region of existence may be shifted in parameter space. We have also found that in situations where the outer solution is favoured by the asymmetry, a new kind of SD appears in the parameter region where a flat wall in 2D becomes modulationally unstable and labyrinthine patterns are formed. These structures are

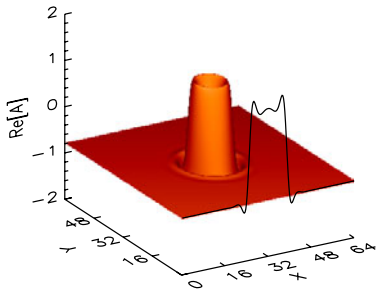

Figure 7. The real part of a stable droplet in the regime of labyrinthine pattern formation for the singly resonant DOPO at $p = 1.935$. Here equation (16) has zero diffusion, $\alpha = 1$, $\mu = -1$, $\nu = 1$, $\beta = 0$, and $\epsilon = 5 \times 10^{-3}$. For these values of the parameters the modulation instability of a flat front is found at $p_c = 2.081$.

nucleation droplets which can be stable as a result of a balance between the asymmetry generated motion of a 1D domain wall and the 2D curvature effect. In the limit $\epsilon \to 0$ these structures continuously transform into the SDs described in [10] which are stabilized by nonlinear curvature effects. Our results have been derived in a completely general context and have been illustrated in a prototypical model like the PCGLE and in the singly resonant DOPO as an example of an optical system. We expect our results to be valid for vectorial Kerr cavities, doubly resonant DOPO, and any system that displays modulational instabilities of an Ising front in the presence of asymmetry of two homogeneous states. In the case of vectorial Kerr cavities, the symmetry breaking can be introduced by a slightly elliptically polarized input beam, and in the DOPO by the injection of a small signal seed [18].

Acknowledgments

We thank A J Scroggie for useful discussions. We acknowledge financial support from the European Commission project QUANTIM (IST-2000-26019). D Gomila acknowledges financial support from EPSRC (Grant No. GR/S28600/01). P Colet and M San Miguel acknowledge financial support from MCyT (Spain) and FEDER under projects BFM2000-1108 (CONOCE) and BFM2001-0341-C02-02 (SINFIBIO). G-L Oppo acknowledges support form SGI, the Royal Society Leverhulme Trust, the PCRI consortium of the University of Strathclyde and EPSRC (Grant No. GR/R04096).

References

[1] Segev M (ed) 2002 *Opt. Photon. News* **13** 27 (Special issue on solitons)
Lugiato L A (ed) 2003 *J. Quantum Electron.* **39** 193 (Feature section on cavity solitons)
[2] Tlidi M, Mandel P and Lefever R 1994 *Phys. Rev. Lett.* **73** 640
Firth W J and Scroggie A J 1996 *Phys. Rev. Lett.* **76** 1623
Coullet P, Riera C and Tresser C 2000 *Phys. Rev. Lett.* **84** 3069
Firth W J and Weiss C O 2002 *Opt. Photon. News* **13** 55
[3] Trillo S, Haelterman M and Sheppard A 1997 *Opt. Lett.* **22** 970
[4] Ouchi K and Fujisaka H 1996 *Phys. Rev.* E **54** 3895
See also Sánchez-Morcillo V J and Staliunas K 1999 *Phys. Rev.* E **60** 6153
[5] Staliunas K and Sánchez-Morcillo V J 1998 *Phys. Rev.* A **57** 1454
[6] Oppo G-L, Scroggie A J and Firth W J 1999 *J. Opt. B: Quantum Semiclass. Opt.* **1** 133
[7] Oppo G-L, Scroggie A J and Firth W J 2001 *Phys. Rev.* E **63** 066209
[8] Le Berre M *et al* 1999 *J. Opt. B: Quantum Semiclass. Opt.* **1** 153
[9] Gallego R, San Miguel M and Toral R 2000 *Phys. Rev.* E **61** 2241
[10] Gomila D, Colet P, Oppo G-L and San Miguel M 2001 *Phys. Rev. Lett.* **87** 194101
[11] Gomila D, Colet P, San Miguel M, Scroggie A J and Oppo G-L 2003 *J. Quantum Electron.* **39** 238
[12] Gunton J D, San Miguel M and Sahni P 1983 *Phase Transitions and Critical Phenomena* vol 8 (New York: Academic) p 269
[13] Petrov V, Ouyang Q and Swinney H L 1997 *Nature* **388** 655
[14] Taranenko V B, Staliunas K and Weiss C O 1998 *Phys. Rev. Lett.* **81** 2236
[15] Peschel U, Michaelis D, Etrich C and Lederer F 1998 *Phys. Rev.* E **58** R2745
[16] Malomed B A and Sakaguchi H 2003 *J. Phys. Soc. Japan* **72** 1360
Barashenkov I V *et al* 2002 *Phys. Rev. Lett.* **89** 104101
[17] Michaelis D *et al* 2001 *Phys. Rev.* E **63** 066602
[18] Rabbiosi I, Scroggie A J and Oppo G-L 2003 *Phys. Rev.* E **68** 036602
[19] Longhi S 1996 *J. Mod. Opt.* **43** 1089
[20] Longhi S 1997 *Phys. Scr.* **56** 611
[21] Sánchez-Morcillo V J, Pérez-Arjona I, Silva F, de Valcarcel G J and Roldan E 2000 *Opt. Lett.* **25** 957
[22] Geddes J B, Moloney J V, Wright E M and Firth W J 1994 *Opt. Commun.* **111** 623
Hoyuelos M, Colet P, San Miguel M and Walgraef D 1998 *Phys. Rev.* E **58** 2292
[23] Elphick C, Hagberg A, Malomed B A and Meron E 1997 *Phys. Lett.* A **230** 33
Coullet P, Lega J and Pomeau Y 1991 *Europhys. Lett.* **15** 221
[24] McSloy J M, Firth W J, Harkness G K and Oppo G-L 2002 *Phys. Rev.* E **66** 046606